Arsenic trioxide induces accumulation of cytotoxic levels of ceramide in acute promyelocytic leukemia and adult T-cell leukemia/lymphoma cells through *de novo* ceramide synthesis and inhibition of glucosylceramide synthase activity

Ghassan S. Dbaibo, Youmna Kfoury, Nadine Darwiche, Shoghag Panjarian, Lina Kozhaya, Rihab Nasr, Mazen Abdallah, Olivier Hermine, Marwan El-Sabban, Hugues de Thé, Ali Bazarbachi

From the Departments of Pediatrics (GSD, SP, LK), Internal Medicine (YK, RN, MA, AB), Biology (ND), and Human Morphology, American University of Beirut, Beirut, Lebanon (ME-S); CNRS UMR 8603 and Department of Hematology, Necker Hospital, Paris, France (OH); UMR 7151 CNRS/University of Paris 7, France (HdT).

Correspondence:
Ali Bazarbachi, MD, Ph.D.
Department of Internal Medicine, American University of Beirut. PO Box 113-6044, Beirut, Lebanon.
E-mail: bazarbac@aub.edu.lb

ABSTRACT

Background and Objectives

Arsenic trioxide (ATO) is an effective treatment for acute promyelocytic leukemia (APL) and potentially for human T-cell leukemia virus type I (HTLV-I) associated adult T-cell leukemia/lymphoma (ATL). Many cytotoxic drugs induce apoptosis through the generation and accumulation of the sphingolipid breakdown product, ceramide, a coordinator of the cellular response to stress. We, therefore, investigated the contribution of ceramide to the mechanism of action of ATO in APL and ATL.

Design and Methods

A human APL-derived cell line (NB4), various ATL-derived lines and an HTLV-I-negative malignant T-cell line were cultured and treated with ATO. Growth and apoptosis assays were conducted. Measurements were made of ceramide, diacylglycerol, sphingomyelinase activity, sphingomyelin mass, glucosylceramide synthase activity and the *de novo* ceramide synthesis.

Results

Treatment of APL and ATL-derived cells with a clinically achievable concentration of ATO induced accumulation of cytotoxic levels of ceramide. The effects of ATO on ceramide levels in APL cells were more potent than those of all-*trans* retinoic acid (ATRA). ATO downregulated neutral sphingomyelinase activity. In contrast to the effect of ATRA, ATO-induced ceramide accumulation was not due to induction of acidic sphingomyelinase, but rather resulted from both *de novo* ceramide synthesis and inhibition of glucosylceramide synthase activity. Interestingly, the effects of ATO on *de novo* ceramide synthesis were similar in APL and ATL-derived cells despite the defective pathway in ATL cells.

Interpretation and Conclusions

These results indicate that ATO-induced ceramide accumulation may represent a general mediator of the effects of ATO, which paves the way for new therapeutic interventions that target the metabolic pathway of this important sphingolipid secondary messenger.

Key words: arsenic trioxide, acute promyelocytic leukemia, adult T-cell leukemia/lymphoma, ceramide synthesis, glycosylceramide synthase.

Arsenic trioxide (ATO) is a very effective treatment for acute promyelocytic leukemia (APL),[1] a distinct subtype of acute myeloid leukemia characterized by unique clinical and laboratory characteristics and a specific cytogenetic abnormality, t(15;17), which results in a reciprocal translocation between the *PML* gene on chromosome 15 and the retinoic acid receptor α (*RAR-α*) gene on chromosome 17.[2,3] Several large randomized and non-randomized trials established that the combination of all-*trans* retinoic acid (ATRA) plus anthracycline-based chemotherapy is the standard treatment for newly diagnosed APL, curing most of the patients.[4-6] Nevertheless, about 20% of patients who attain a complete remission will eventually relapse. Initial reports from China showed that APL patients resistant to ATRA and chemotherapy could still respond to ATO.[7] Other studies confirmed these findings and showed that ATO is more efficient than ATRA in reducing the degree of minimal residual APL cells.[1,8,9] The high complete remission rate with ATO in relapsed APL led to investigation of the efficacy of this drug in newly diagnosed patients. Animal and human studies using ATO, either alone or combined with ATRA, suggest that patients with newly diagnosed APL can potentially be cured without or with only minimal use of chemotherapy.[10-13] At the cellular level, *in vitro* studies on an APL-derived cell line (NB4) showed that ATO triggers relatively specific NB4-cell apoptosis at micromolar concentrations.[14] Lower doses of arsenic were shown to induce differentiation of the leukemic cells.[14] At the molecular level, ATO specifically leads to the degradation of the PML/RARα oncoprotein.[15] Adult T-cell leukemia/lymphoma (ATL) is an aggressive lymphoid proliferation of mature, activated CD4+ T lymphocytes, secondary to infection by the human T-cell leukemia virus type I (HTLV-I).[16] The treatment of ATL remains disappointing, with a median survival of 6 to 8 months in the acute form.[17,18] This very poor prognosis is due to an intrinsic resistance of leukemic cells to chemotherapy and to an associated severe immunosuppression. High response rates were achieved with the combination of the antiretroviral nucleotide analog zidovudine and interferon-α.[19-22] However, most patients eventually relapse, which underlines the need for new therapeutic approaches. We have shown that ATO synergizes with interferon-α to induce cell cycle arrest and apoptosis in ATL.[23] At the molecular level, this combination specifically induces proteosomal degradation of the HTLV-I oncoprotein Tax and reversal of NF-κB activation.[24,25] The results of a phase II clinical trial in relapsed/refractory ATL patients, previously treated with an interferon-containing regimen, demonstrates that ATO has striking anti-leukemic effects.[26]

One of the apoptotic mechanisms induced by cytotoxic drugs is mediated through the generation and accumulation of the sphingolipid breakdown product, ceramide, which was recently proposed as a co-ordinator of the cellular response to stress.[27,28] Endogenous levels of ceramide are increased in response to treatment with different chemotherapeutic agents, cytokines, or other cell stressors.

Defects in ceramide production render cells more resistant to killing by these inducers,[29,30] while elevation of endogenous ceramide levels lowers the threshold for apoptosis induction by these agents.[31,32] Cell permeable ceramide analogs can also reproduce the growth suppressive effects of these inducers.[33] At the molecular level, ceramide accumulation is usually the result of sphingomyelin breakdown or *de novo* ceramide synthesis, and sometimes the inhibition of ceramide clearance through sphingomyelin synthase, glucosylceramide synthase, or ceramidases.[34,35]

Murate *et al.*[36] reported that ATRA treatment of NB4 APL cells results in upregulation of acidic sphingomyelinase (A-smase) and an increase in intracellular levels of ceramide. Darwiche *et al.*[37] recently showed that HTLV-I-transformed cells have a partial defect in ceramide synthesis, which renders them less sensitive to N-(4-hydroxyphenyl) retinamide. In this report, we investigated the contribution of ceramide in the mechanism of action of ATO in APL and ATL.

Design and Methods

Cell lines, drugs and culture conditions

The HTLV-I-transformed CD4+ T cell lines (HuT-102, MT-2, C91-PL) and HTLV-I-negative malignant T cells (CEM) were cultured as previously described.[37] NB4, a human APL cell line,[38] was grown in RPMI 1640 medium containing 10% heat-inactivated fetal bovine serum (FBS) and antibiotics (Gibco-BRL, Baithersburg, MD, USA). Cells were cultured for 24 h at a concentration of 2×10^5 cells/mL, unless indicated otherwise. ATO (Sigma Chemical Co, St Louis, MO, USA) and recombinant interferon-α (Hoffman-La Roche, Basel, Switzerland) were used at the concentration of 1 μM and 1000 U/mL, respectively, as previously described.[23] ATRA was used at a final concentration of 1 μM in dimethylsulfoxide (DMSO). The short chain cell-permeable ceramides C2- and C6-ceramides (Biomol, Plymouth Meeting, PA, USA) were used at final concentrations ranging from 1 μM to 20 μM in 100% pure ethanol. Prior to ceramide treatment, cells were cultured in RPMI 1640 medium containing 2% FBS. The inhibitor of ceramide synthase, myriocin, was purchased from Biomol and used at a concentration of 50 nM.

Growth and apoptosis assays

Cell growth was assessed by cell count using trypan blue dye exclusion protocols and/or the CellTiter 96® non-radioactive cell proliferation assay kit (Promega Corp., Madison, WI, USA) as suggested by the manufacturer. Results are expressed as cell growth relative to DMSO-treated controls and are derived from the mean of triplicate wells. Apoptosis was assessed by measuring the percentage of cells with shrunken and intensely-fluorescent nuclei. Briefly, nuclei were labeled by Hoechst 33258 (Polysciences, Warrington, PA, USA) for 2 min at room temperature. Cells were then observed under fluorescence microscopy using an ultraviolet light filter pack.

Ceramide and diacylglycerol measurement

Ceramide was measured with a modified diacylglycerol kinase assay using external ceramide standards as described elsewhere.[39,40] Briefly, dried lipid was solubilized in 7.5% octyl-β-D-glucoside, 25 mM dioleoyl phosphatidylglycerol solution. Reaction buffer was added to the lipid micelles, and the reaction was started by adding [γ-^{32}P] ATP solution and allowed to proceed at 25°C for 30 minutes. Lipid extracts were resuspended in methanol/chloroform (1:9, v/v) and spotted on silica gel thin layer chromatography plates. The plates were developed with chloroform:acetone:methanol:acetic acid:H$_2$O (50:20:15:10:5), air-dried, and subjected to autoradiography. The radioactive spots corresponding to phosphatidic acid and ceramide-phosphate (the phosphorylated products of diacylglycerol and ceramide, respectively) were identified by comparison to known standards, scraped and counted on a scintillation counter. Linear curves of phosphorylation were produced over a concentration range of 0-960 pM of external standards (dioleoyl glycerol and CIII ceramide; Sigma). Ceramide levels were always normalized to lipid phosphate levels.

Sphingomyelinase activity

Cells were sonicated for 30 s in the lysis buffer containing 0.25 M sucrose, 10 mM Hepes, 50 mM Tris HCL pH=7.4, 0.001% TritonX, 500 mM PMSF, and 1 X Complete Protease inhibitors cocktail from Roche, (Mannheim, Germany). The resultant homogenate was used for the assay of sphingomyelinase activity which is measured by the formation of radioactive phosphocholine from [N-methyl-^{14}C] sphingomyelin from Perkin Elmer (Boston, MA, USA).

The assay mixture for A-smase contained 8.5 μL ^{14}C-labeled sphingomyelin from a 0.02 mCi stock and 0.07 mg/mL cold sphingomyelin Avanti Polar Lipids (Alabaster, AL, USA). Subsequently, this latter mixture was dried and resuspended in 0.1 M sodium acetate, 0.1% Triton and 50 μg of total cellular proteins in a total volume of 100 μL and incubated for 30 min at 37°C. This assay mixture also contained 8.5 μL ^{14}C-labeled sphingomyelin from a 0.02 mCi stock, 0.07 mg/mL cold sphingomyelin, and 0.15 mg/mL phosphatidylcholine.

The assay mixture for Mg^{++}-dependent N-smase contained 0.05% Triton, 0.05 M Tris, 0.005 M DTT, 0.005 M MgCl$_2$, and 50 μg of total cellular proteins in a total volume of 100 μL and was incubated for 45 min at 37°C. After incubation, all S-mase reaction mixtures were terminated by the addition of 1.5 mL of chloroform/methanol (2:1, v/v); the phases were separated after addition of 200 μL of water. After centrifugation, the radioactivity of phosphocholine recovered from 300 μL of the upper phase layer was mixed with 4 mL of scintillation fluid (Perkin Elmer, Boston, MA, USA) for liquid scintillation counting.

Sphingomyelin mass measurement

Cells were washed in ice-cold phosphate-buffered saline, centrifuged and the pellet formed resuspended in 2 mL methanol and 1 mL chloroform and then stored at -80°C. Lipids were extracted in 1 mL chloroform and 1 mL water, and then centrifuged; subsequently, the lower phase was collected and the chloroform evaporated. The pellet was resuspended in chloroform. For the measurement of sphingomyelin, the lipids in chloroform were mixed with the same volume of 2 N NaOH in methanol and incubated at 37°C for 1.5 h. Samples were neutralized by the addition of a 0.2 volume of 0.5 N HCl in methanol. Lipids were separated by thin layer chromatography (TLC) in solvent (chloroform, methanol, acetic acid, 50:30:8) and visualized with iodine vapor. Bands corresponding to sphingomyelin were scraped, lipids were extracted from the silica gel, and the mass of lipid phosphate was determined as described elsewhere.[41]

Glucosylceramide synthase activity

The conversion of NBD (12-(N-methyl-N-(7-nitrobenz-2-oxa-1,3-diazol-4-yl))-C$_6$-ceramide to NBD-C$_6$-glucosylceramide was detected in cell extracts at 37°C for 90 min in the presence of UDP-glucose as described previously.[42] The final products were separated on TLC plates and observed under a UV source. Cells were homogenized by centrifugation in lysis buffer (25 mM Tris-HCl, pH 7.4, 0.25 mM EDTA, 12.5 mM KCl). The enzyme reaction contained 0.025 mM NBD-C$_6$-ceramide (Molecular Probes, Netherlands), 0.0425 mg/mL phosphatidylcholine and 0.6 mM UDP-glucose. The glucosylceramide substrate was prepared by mixing all components to 150 μg of cellular proteins, evaporating solvents under a stream of nitrogen and sonicating on ice for 1 min. The reaction was terminated by adding 1 mL of methanol, 1 mL of chloroform and 400 μL of H$_2$O. Briefly, samples were vortexed, centrifuged and the lower phase was dried in a tube. The pellet was resuspended in chloroform and separated on a TLC plate in solvent containing 120 mL chloroform, 70 mL methanol and 15 mM CaCl$_2$. Bands were quantified using the phosphoimager Molecular Dynamics Storm 860 System (Molecular Dynamics, Sunnyvale, CA, USA).

De novo ceramide synthesis

At initiation of treatment, [^{3}H]palmitic acid (1 μCi/mL medium) purchased from Perkin Elmer was added to treated and control samples. Extracted lipids, dried under N$_2$ were resuspended in 60 μL chloroform:methanol (2:1) and 40 μL were spotted on 20 cm silica gel TLC plates. Plates were developed with ethylacetate:isooctane:acetic acid (90:50:20, v/v), air dried, and sprayed lightly with En^{3}hance® (Perkin Elmer) to enhance tritium readings. Radioactivity was visualized by autoradiography and [^{3}H] ceramide spots were scraped in scintillation vials containing 4 mL of scintillation fluid and then counted with a Packard scintillation counter. [^{3}H] ceramide counts were normalized to lipid phosphate levels.
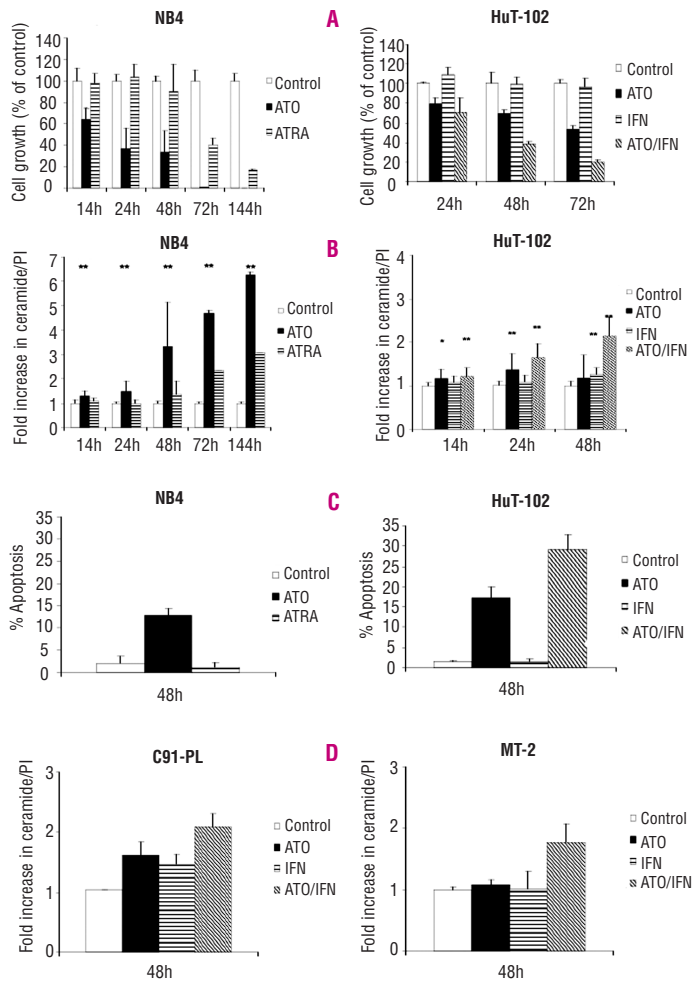
Figure 1. Arsenic trioxide induces ceramide accumulation in APL- and ATL- derived cells. **A-C.** ATO inhibits growth of APL- derived cells and synergizes with interferon-α (IFN) to induce cell cycle arrest and apoptosis in ATL- derived cells: NB4 cells were seeded at 2×10^5 cells/mL and treated with 0.1% DMSO (control), 1 μM ATO or 1 μM ATRA for the indicated time-points. HuT-102 cells were seeded at 2×10^5 cells/mL and treated with 1 μM ATO, 1000 U/mL IFN or combined IFN for the times indicated. **A.** Cell growth was assayed in triplicate wells using the Cell Titer 96® non-radioactive cell proliferation kit. Results are expressed as percentage of control. **C.** Cells were stained with Hoescht 333258. Apoptosis was assessed by measuring the percentage of cells with shrunken and intensely-fluorescent nuclei. **B,D.** ATO and ATRA result in a progressive increase of intracellular ceramide levels in APL-derived cells and the combination of ATO and IFN results in a synergistic increase in intracellular ceramide in ATL-derived cells: NB4 cells were seeded at 2×10^5 cells/mL and treated with 0.1% DMSO (control), 1 μM ATO or 1 μM ATRA for the times indicated. HuT-102, C91-Pl and MT-2 cells were seeded at 2×10^5 cells/mL and treated with 1 μM ATO, 1000U/mL IFN or the combination of ATO and IFN for the times indicated. Ceramide levels were determined in triplicate using the DGK assay as described in the Materials and Methods section and normalized to total cellular inorganic phosphate (Pi) levels. Data points represent the mean ± (SD). Results are representative of at least three independent experiments. The asterisks * and ** indicate statistically significant differences ($p \leq 0.05$ or $p \leq 0.01$, respectively) versus control using the *t*-test.

Statistical analysis

The significance of the observed results was assessed using the two-sample Student's *t*-test.

Results

ATO induces ceramide accumulation in APL and ATL-derived cells

The established role of ceramide in regulating cell growth and cell death led us to assess the contribution of ceramide in the mechanism of action of ATO in APL and ATL-derived cells. As previously reported, treatment of the APL-derived cell line NB4 with ATO resulted in a significant decrease of cell growth, which was present as early as 14 h, and reached 70% inhibition by 48 h (Figure 1A). In contrast, ATRA treatment had no significant effect on the growth of NB4 cells at these early time points. Long-term treatment of NB4 cells with ATO or ATRA resulted in 100% and 85% inhibition of cell growth, respectively, by day 6 Figure 1A). Similarly, treatment of the ATL-derived cell line HuT-102 with ATO reduced cell growth by 50% at 72 h. (Figure 1A). As previously reported,[23] this effect was significantly enhanced by the addition of interferon-α, resulting in growth inhibition to 20% of control by 72 h, while interferon-α alone had no significant effect. Similar

results were observed with the HTLV-I transformed MT-2 and C91-PL cell lines (*data not shown*). We then examined the effects of ATO on cellular ceramide in APL and ATL-derived cells. Ceramide levels were first measured in NB4 cells treated with ATO or ATRA (Figure 1B). As previously reported, ATRA treatment resulted in a progressive increase in intracellular ceramide levels. This increase started at 48 h and the levels became more than 3-fold higher than control levels at 6 days ($p<0.01$). Similarly, ATO treatment increased intracellular ceramide. Interestingly, the effects of ATO on ceramide levels were more potent than those of ATRA. Indeed, endogenous ceramide started to increase as early as 14 h in ATO-treated NB4 cells (130% of the control; $p<0.01$), reached levels more than 3 to 4-fold higher than control levels by 48 h and 72 h, respectively ($p<0.01$), and continued to increase to more than 6-fold by day 6 of treatment ($p<0.01$). Ceramide levels were also measured in the HTLV-I transformed cell lines, HuT-102, MT-2 and C91-PL treated with ATO, interferon-α, or their combination at the indicated time points (Figure 1B). In HuT-102 cells, levels of ceramide increased moderately but significantly by 14 h (120% of the control; $p<0.05$) with ATO treatment and continued to increase at 24 h reaching 140% of the control ($p<0.05$). Although interferon-α had no significant effects on ceramide levels when used alone,

its combination with ATO resulted in a significant synergistic increase, particularly at 48 h following treatment, producing levels around 200% of those in untreated control cell lines ($p<0.01$). It is noteworthy that the ATO-induced increase in intracellular ceramide levels in NB4 cells was more dramatic than that observed in HuT-102, in agreement with the higher sensitivity of NB4 cells to ATO. Although following the same trend as cell growth inhibition, the ATO-induced increase of intracellular ceramide levels in NB4 and HuT-102 cells was less dramatic than the observed cell growth inhibition, particularly at early time points. Since ATO-mediated growth inhibition results from both cell cycle arrest and apoptosis,[23] we measured the percentage of apoptotic cells using Hoechst nuclear staining. We found that, at 48 h, ATO induced apoptosis in 13% and 17% of NB4 and HuT-102 cells, and that combined ATO/interferon treatment induced apoptosis in 28% of HuT-102 cells (Figure 1C). ATRA alone and interferon alone did not induce apoptosis of NB4 and HuT-102 cells, respectively. These results are in agreement with ceramide accumulation. Results in C91-PL cells were similar to those observed in HuT-102 cells (Figure 1D). Finally, in MT-2 cells, ceramide accumulation (180% of control) was only observed following combined treatment with ATO and interferon (Figure 1D). This ceramide accumulation is again in agreement with the effects of ATO and/or interferon on the growth inhibition of these cells.[23] Collectively, these results indicate that ATO induces ceramide accumulation in both APL and ATL-derived cells with a potent synergy with interferon in HTLV-I transformed cells.

Exogenous ceramides induce cell death in APL and ATL-derived cells

To demonstrate the specificity of ATO-induced ceramide accumulation, we compared the effects of ATO/interferon in HuT-102 cells and in the HTLV-I-negative malignant T cells, CEM. As previously reported,[23] CEM cells are resistant to treatment with ATO/interferon, which had a minimal effect on their growth at 48 h (Figure 2A). Importantly, ATO/interferon treatment for 48 h resulted in minimal non-significant changes in intracellular ceramide levels in CEM cells (Figure 2B), further demonstrating that ATO-induced ceramide accumulation correlates with cell growth inhibition and apoptosis. In order to explore the role of the accumulated ceramide in response to ATO, NB4 cells were treated with synthetic, cell-permeable, short-chain ceramide N-acetylsphingosine (C2-ceramide) or N-hexanoylsphingosine (C6-ceramide). Increasing concentrations of C2- or C6-ceramide significantly reduced the growth of these cells in a dose- and time-dependent manner. While a 1 µM concentration of either C2 or C6-ceramide had a moderate effect on NB4 growth, a 5 µM concentration of C2-ceramide or C6-ceramide reduced growth to 44% and 23% of control levels, respectively, at 48 h, and a 10 µM concentration of C2-ceramide or C6-ceramide further reduced this cell growth to 3% and 11% of control levels, respectively, at 48 h (Figure 2C). When HuT-102 cells were
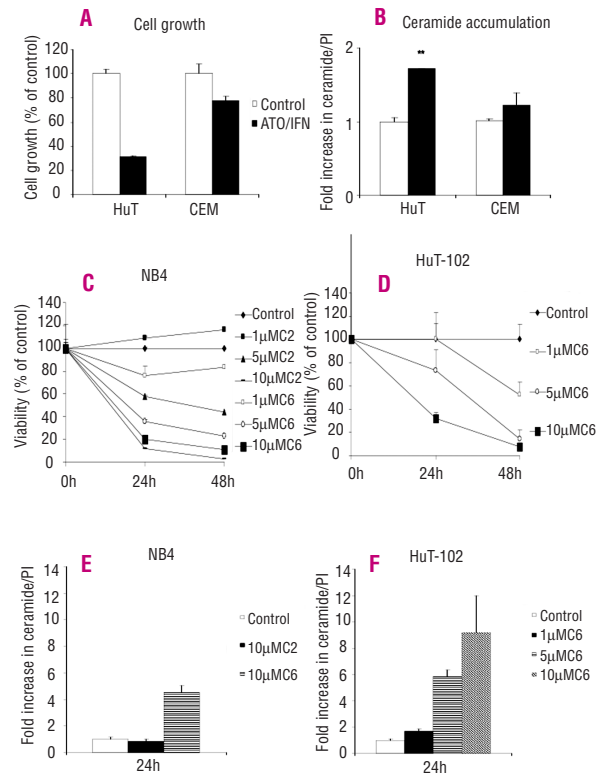

Figure 2. Arsenic trioxide-induced ceramide accumulation correlates with growth inhibition. **A.** ATO synergizes with interferon-α (IFN) to induce growth inhibition of HTLV-I positive but not HTLV-I negative malignant T cells: HuT-102 and CEM cells were seeded at 2×10^5 cells/mL and treated with 1 µM ATO, 1000 U/mL IFN or combined ATO/IFN for the times indicated. Cell growth was assayed in triplicate wells using the Cell Titer 96® non-radioactive cell proliferation kit. Results are expressed as percentage of control. **B.** ATO and IFN result in a synergistic increase in intracellular ceramide in ATL-derived cell but not in HTLV-I-negative malignant T cells: HuT-102 and CEM cells were seeded at $2x10^5$ cells/mL and treated with 1 µM ATO, 1000 U/mL IFN or the combination of ATO/IFN for the times indicated. Ceramide levels were determined in triplicate using the DGK assay as described in the Materials and Methods section and normalized to total cellular inorganic phosphate (Pi) levels. Data points represent the mean ± (SD). **C, D.** C6-Ceramide and C2-Ceramide inhibit growth of APL- and ATL-derived cells: NB4 cells (**C**) were seeded at 2×10^5 cells/mL and treated with 0.1% ethanol (control), C2-Ceramide (1 µM, 5 µM, 10 µM), or C6-Ceramide (1 µM, 5 µM, 10 µM) for the times indicated. HuT-102 cells (**D**) were seeded at 2×10^5 cells/mL and treated with 0.1% ethanol (control), or C6-Ceramide (1 µM, 5 µM, 10 µM) for the times indicated. Cell growth was assayed in triplicate wells using the Cell Titer 96® non-radioactive cell proliferation kit. The results are expressed as a percentage of 0.1% ethanol control. **E, F.** C6-Ceramide induces the accumulation of endogenous ceramide levels in APL- and ATL-derived cells: NB4 cells (**E**) were seeded at 2×10^5 cells/mL and treated with 0.1% ethanol as a control, 10 µM C2-Ceramide or C6-Ceramide for the times indicated. HuT-102 cells (**F**) were seeded at 2×10^5 cells/mL and treated with 0.1% ethanol as control or C6-Ceramide (1 µM, 5 µM, 10 µM) for the times indicated. Ceramide levels were determined in triplicate using the DGK assay as described in the Design and Methods section and normalized to total cellular lipid Pi levels. Data points represent the mean ± (SD).

treated for 48 h with 1 µM, 5 µM or 10 µM C6-ceramide, their growth was reduced to 52%, 14%, and 8% of control levels, respectively (Figure 2D). Similar results were observed with MT-2 cells (*data not shown*). Finally, treatment of HuT-102 cells with C2-ceramide also induced a dose- and time-dependent growth inhibition.[37] The mechanisms of action of C2- and C6-ceramide differ.[43] C2-ceramide functions mostly as an analog of endogenous
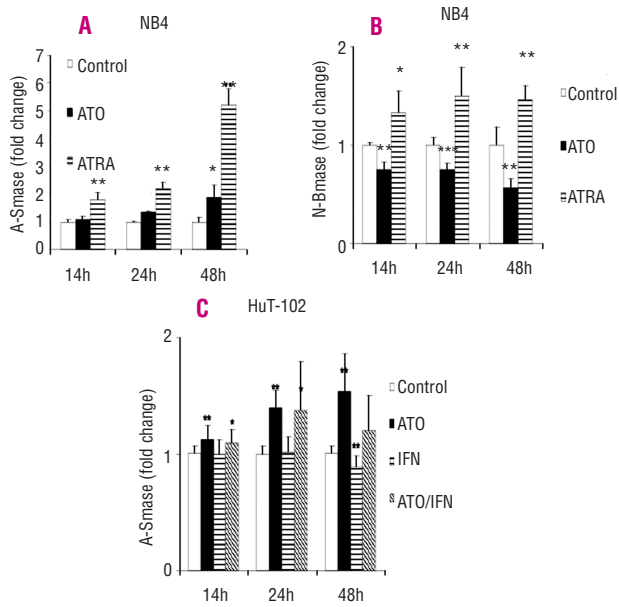
Figure 3. Arsenic trioxide-induced ceramide accumulation is not due to sphingomyelinase induction. (A,C) ATO induces A-smase in APL and ATL cells. NB4 cells (A) were seeded at 2×10⁵ cells/mL and treated with 0.1% DMSO (control), 1 μM ATO or 1 μM ATRA for the times indicated. Hut-102 cells (C) were seeded at 2×10⁵ cells/mL and treated with 1 μM ATO, 1000 U/mL interferon (IFN) or combined ATO/IFN for the times indicated. Acidic sphingomyelinase (A-smase) activity was determined in triplicate as described in the *Design and Methods* section using 50 μg of total cellular proteins. Data points represent the mean ± (SD). Results are expressed as fold change in A-smase over the control set as one. Results are representative of at least three independent experiments. The asterisks * and ** indicate statistically significant (*p*≤0.05 or *p*≤0.01 respectively) differences using the t-test. B. ATO inhibits N-smase in APL cells. NB4 cells were seeded at 2×10⁵ cells/mL and treated with 0.1% DMSO (control), 1 μM ATO or 1 μM ATRA for the times indicated. Neutral Mg²⁺-dependent sphingomyelinase (N-smase) activity was determined in triplicate as described in the *Design and Methods* section using 50 μg of total cellular proteins. Data points represent the mean ± (SD). Results are expressed as fold change in N-smase over the control set as one. Results are representative of at least three independent experiments. The asterisks * and ** indicate statistically significant (*p*≤0.05 or *p*≤0.01, respectively) differences using the t-test.

Figure 4. Arsenic trioxide induces sphingomyelin accumulation and decreases diacylglycerol levels in APL- and ATL- derived cells (A,B) ATO increases sphingomyelin mass in APL and ATL cells. NB4 cells (A) were seeded at 2×10⁵ cells/mL cellular density and treated with 0.1% DMSO (control), 1 μM ATO or 1 μM ATRA for the 48 hours. HuT-102 cells were seeded at 2×10⁵ cells/mL and treated with 1 μM As, 1000 U/mL IFN or combined ATO/IFN for 48 hours. Sphingomyelin mass was determined in triplicates as described in the *Design and Methods* section and was normalized to total cellular lipid Pi levels. Data points represent the mean ± (SD). Results are expressed as fold change in sphingomyelin mass over control set as one. (C,D) Arsenic trioxide decreases DAG levels in APL and ATL cells. NB4 cells (C) were seeded at 2×10⁵ cells/mL and treated with 0.1% DMSO (control), 1 μM ATO or 1 μM ATRA for 48 hours. HuT-102 cells (D) were seeded at 2×10⁵ cells/mL and treated with combined ATO/IFN for 48 hours. DAG was determined in triplicate using the DGK assay as described in the *Design and Methods* section and normalized to total cellular lipid Pi levels. Data points represent the mean ± (SD). Results are expressed as fold change in DAG over the control set as one.

5 μM and 10 μM C6-Ceramide, respectively (Figure 2F). These studies indicate that exogenous ceramides could reproduce the effects of ATO on APL and ATL-derived cells either by functioning directly or by inducing the generation of endogenous ceramides, suggesting that ceramide accumulation may mediate some of the observed effects of ATO on cell growth and apoptosis.

ATO-induced ceramide accumulation is not due to induction of sphingomyelinase activity

Several mechanisms regulate the accumulation of ceramide in response to various inducers. One of the major pathways of generation of cellular ceramides is through the action of one or more sphingomyelinases, specialized phospholipases that preferentially hydrolyse membrane sphingomyelin to generate ceramide and choline phosphate. The two major sphingomyelinases implicated in ceramide generation in response to various agonists are acidic sphingomyelinase (A-smase) with preferential lysosomal localization and some evidence of cell membrane localization, and the neutral magnesium-dependent sphingomyelinase (N-smase) with preferential membrane localization. The activity of A-smase and N-smase in response to ATO or ATRA was measured in NB4 cells (Figure 3A). As previously reported, ATRA treatment resulted in a strong activation of A-smase starting at 14 h and reaching a 5-fold increase over control at 48 h (*p*<0.01). In contrast,

ceramides, whereas C6-ceramide functions both directly as an analog, and indirectly by inducing the generation of endogenous ceramides through a deacylation-reacylation reaction dependent on ceramide synthases. We measured the levels of endogenous ceramides in NB4 and HuT-102 cells following C2- and C6-ceramide treatment. In NB4 cells, treatment with C2-ceramide for 24 h did not induce endogenous ceramide synthesis, as expected, whereas treatment with C6-ceramide under the same conditions resulted in significant generation of endogenous ceramides reaching a 4.5 fold increase over control levels (Figure 2E). In HuT-102 cells, treatment with C6-ceramide at a concentration of 1 μM, which inhibits the growth of these cells in a similar manner to that of ATO, resulted in the accumulation of endogenous ceramide, reaching 160% of control levels at 24 h. It is noteworthy that these levels are quite comparable to those generated by ATO treatment of these cells (Figure 2F). Higher concentrations of C6-ceramide resulted in further increases of endogenous ceramide levels reaching 6-fold and 9-fold increases over control levels with
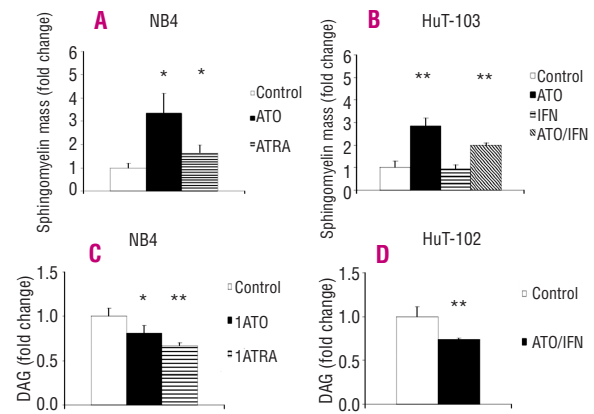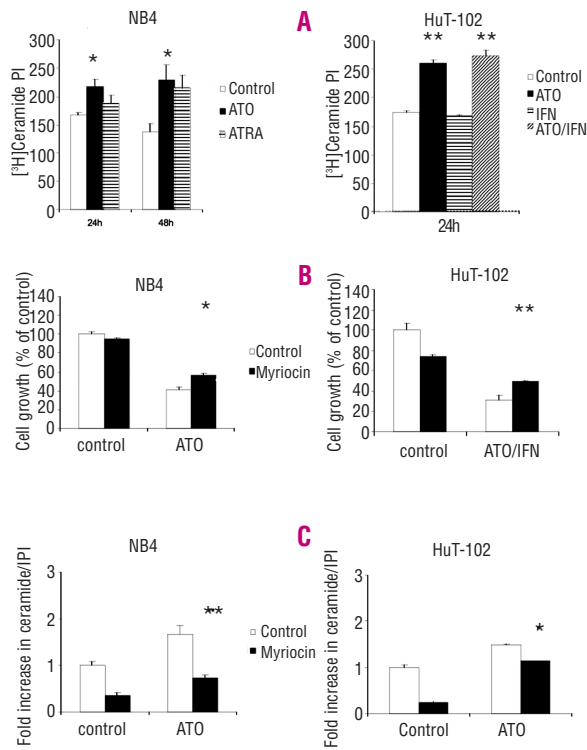
Figure 5. Arsenic trioxide induces *de novo* ceramide synthesis in APL and ATL cells. NB4 cells were seeded at 2×10⁵ cells/mL and treated with 0.1% DMSO (control), 1 μM ATO, 1 μM ATRA for 24 and 48 hours. HuT-102 cells were seeded at 2×10⁵ cells/mL and treated with 1 μM ATO, 1000 U/mL IFN or combined ATO/IFN for 24 hours. **A.** *De novo* ceramide levels were determined in triplicate using the [³H] palmitate incorporation method as described in the *Design and Methods* section and normalized to total cellular lipid Pi levels. Data points represent the mean ± (SD). **B.** Cells were treated with the ceramide synthase inhibitor, myriocin. Cell growth was assayed in triplicate wells using the Cell Titer 96® non-radioactive cell proliferation kit. Results are expressed as a percentage of control. The asterisks * and ** indicate statistically significant differences (*p*≤0.05 or *p*≤0.01, respectively) versus the control using the *t*-test. **C.** Cells were treated with the ceramide synthase inhibitor, myriocin. Ceramide levels were determined in triplicate using the DGK assay as described in the *Design and Methods* section and normalized to total cellular inorganic phosphate (Pi) levels. Data points represent the mean ± (SD). The asterisks * and ** indicate statistically significant differences (*p*≤0.05 or *p*≤0.01, respectively) versus the control using the *t*-test.

Figure 6. Arsenic trioxide inhibits glucosylceramide synthase activity in APL and ATL cells. NB4 cells (**A**) were seeded at 2×10⁵ cells/mL and treated with 0.1% DMSO (control), 1 μM ATO, 1 μM ATRA for 48 hours. HuT-102 (**B**) cells were seeded at 2×10⁵ cells/mL and treated with 1 μM ATO for 48 hours. Glucosylceramide synthase (GCS) activity was determined in triplicate using NBDC6 ceramide and 50 μg of total cellular proteins as described in the *Design and Methods* section. Results are expressed as fold change in GCS activity over the control set as one. Data points represent the mean ± (SD) and are representative of at least three independent experiments. The asterisks ** indicate statistically significant (*p*≤0.05) difference using the *t*-test.

ATO treatment resulted in a more moderate activation of A-smase with a ~190% increase over control at 48 h (*p*<0.05). Hence, activation of A-smase did not correlate with the increase of ceramide levels in response to the corresponding treatments (compare with Figure 1). On the other hand, ATO caused a significant decrease in the activity of N-smase by ~20% at 14 and 24 h (*p*<0.05 and 0.01, respectively), and by ~40% at 48 h (*p*<0.05), whereas ATRA induced a significant increase of N-smase activity by 150% of control levels at these time points (*p*<0.05) (Figure 3B). Again, there was no correlation between the changes in N-smase activity and the accumulated ceramide in response to ATO or ATRA in these cells (compare with Figure 1).

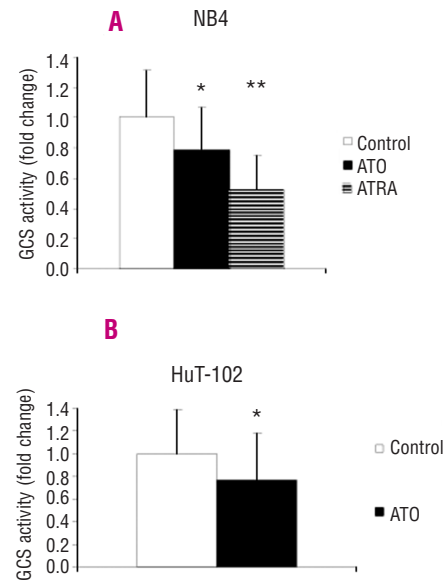The activity of A-smase was also measured in ATO-treated HuT-102 cells (Figure 3C). Minimal, but statistically significant, A-smase activation was observed starting at 14 h in these cells in response to ATO, and reaching a ~ 150% (*p*<0.01) increase in activity at 48 h. Surprisingly, addition of interferon appeared to attenuate this activation to ~ 90% that of the control (*p*<0.01), which did not correlate with the levels of ceramide generated by the same treatment (compare with Figure 1). Finally, basal N-smase activity was very low in HuT-102 cells and did not change in response to ATO (*data not shown*). Collectively, these studies indicate that, unlike ATRA, ATO-induced ceramide generation is not or only partially dependent on smase activation.

In order to verify whether the changes in activity of smases in response to ATO were associated with changes in their substrate, sphingomyelin, we measured sphingomyelin mass in response to ATO in both cell lines. In NB4 cells, ATO treatment significantly increased sphingomyelin mass under conditions in which A-smase activity was increased but N-smase activity was inhibited. At 48 h, ATO increased the sphingomyelin mass to ~3.5-fold over the control, whereas minimal changes were seen with ATRA (Figure 4A). Similarly, in HuT-102 cells, sphingomyelin mass increased in response to ATO to ~3-fold over the control, levels under the same conditions in which A-smase was activated (Figure 4B). Indeed, sphingomyelin mass is determined by the balance of its hydrolysis by sphingomyelinases and its synthesis by sphingomyelin synthases. The synthesis of sphingomyelin from ceramide

and phosphatidylcholine is mediated by the action of sphingomyelin synthases and produces sphingomyelin and diacylglycerol. Thus, if sphingomyelin synthase were activated by ATO to produce the observed increase in sphingomyelin mass, diacylglycerol levels would be expected to increase. However, when diacylglycerol levels were measured in response to ATO, it was found that they actually decreased in both cell lines (Figure 4). Treatment of NB4 cells with ATO for 48 h led to a decrease in diacylglycerol levels to 80% of control levels (Figure 4C). Similarly, treatment of HuT-102 cells with the combination of ATO and interferon led to a decrease in diacylglycerol to 75% of control values (Figure 4D). These findings indicate that the ATO-induced increase in sphingomyelin mass was unlikely to be due to enhanced sphingomyelin synthesis by ATO, but more likely resulted from the inhibition of N-smase activity, at least in NB4 cells. More importantly, they confirm that the generation of ceramide in response to ATO is not due to smase activation and sphingomyelin hydrolysis.

ATO-induced ceramide accumulation is associated with de novo ceramide synthesis and inhibition of glucosylceramide synthase activity

The second major pathway by which cellular ceramide levels are increased is by *de novo* ceramide synthesis from serine and palmitate. We assessed *de novo* ceramide synthesis by measuring the incorporation of radiolabeled palmitate in newly synthesized ceramide. In NB4 cells, both ATO and ATRA treatments increased the incorporation of radiolabeled palmitate to 165% and 155% of control values, respectively (Figure 5A). Similarly, in HuT-102 cells, ATO and ATO/interferon, but not interferon alone, increased the incorporation of radiolabeled palmitate to 155% and 150% of control values, respectively (Figure 5B). To confirm the implication of *de novo* ceramide synthesis with regards to the effects of ATO, we used the inhibitor of serine palmitoyl transferase, myriocin, which blocks the first step of *de novo* ceramide synthesis. We found, in both NB4 and HuT-102 cell lines, that myriocin treatment resulted in a partial, but significant, protective effect on both ATO-induced growth inhibition (Figure 5B) and the ATO-mediated increase in intracellular ceramide levels (Figure 5C). Collectively, these findings indicate that *de novo* synthesis contributes to the increase in ceramide levels in response to ATO and that ATO-induced ceramide accumulation contributes to the observed growth inhibition. Another recently described pathway of increasing cellular ceramide levels is the inhibition of glucosylceramide synthase (GCS). This enzyme catalyzes the first step in the synthesis of a large variety of complex glycosphingolipids, and its inhibition results in the accumulation of ceramide that would have otherwise been metabolized to these abundant lipids. Treatment of NB4 and HuT-102 cells with ATO inhibited GCS activity by 30% ($p<0.05$) and 40% ($p<0.05$), respectively (Figure 6). Similarly, ATRA treatment of NB4 cells inhibited GCS activity by 50% ($p<0.05$) (Figure

6A). These findings suggest that inhibition of GCS by ATO also contributes to the observed accumulation of ceramide.

Discussion

In this study, we showed that ATO treatment of APL and ATL-derived cells resulted in the accumulation of cytotoxic levels of the sphingolipid breakdown product, ceramide. This ceramide accumulation is due to *de novo* ceramide synthesis and inhibition of ceramide metabolism. In a variety of cell types, ceramide has several growth suppressive effects including induction of differentiation,[44] induction of Rb dephosphorylation with resultant cell cycle arrest in G_0/G_1,[45,46] induction of apoptosis,[47] and senescence.[48] Endogenous levels of ceramide are increased in response to treatment with different chemotherapeutic agents, cytokines, or other cell stressors. Inducers of ceramide accumulation include tumor necrosis factor-α, Fas ligand, interleukin-1, γ-interferon, CD28 ligation, complement, serum deprivation, γ-irradiation, heat shock, ultraviolet radiation, and most chemotherapeutic agents examined.[49]

In APL cells, Murate *et al*.[36] reported transcriptional upregulation of A-smase during ATRA-induced myeloid differentiation of parental NB4 cells but not NB4/RA cells, a subclone harboring a point mutation in the *RARα* gene that renders cells resistant to ATRA. This upregulation of A-smase resulted in ceramide accumulation. In this study, we show that, in addition, ATRA induces *de novo* synthesis of ceramide in NB4 cells. Interestingly, we found that, compared to ATRA, ATO induced a faster and significantly more robust ceramide accumulation in NB4 cells. This likely explains the greater ability of ATO to induce *in vitro* NB4 cell apoptosis, particularly in view of the fact that cell-permeable ceramide analogs also had growth suppressive effects on NB4 cells.

In APL cells, the molecular mechanisms of ATO-induced and ATRA-induced ceramide accumulation differ. The extent of ATO-induced A-smase induction was significantly lower than that induced by ATRA, despite higher levels of ceramide generation. In the case of ATO, this activation was not involved in the generation of the bulk of ceramide which occurred much earlier. Also, ATO significantly downregulated N-smase activity whereas ATRA induced it. Furthermore, combined ATO/ATRA treatment of NB4 cells also suppressed N-smase activity (*data not shown*). The finding that sphingomyelin mass, the substrate of sphingomyelinase, actually increased in response to ATO, confirmed that sphingomyelin turnover was not the source of ceramide generation. Moreover, the increase in sphingomyelin mass was not associated with the generation of diacylglycerol, the byproduct of the reaction catalyzed by sphingomyelin synthase. This suggests that the increase in sphingomyelin mass was not because of new synthesis but due to decreased turnover, probably as a result of the inhibition of N-smase activity to levels below control ones.

The significance of this is, however, unknown.

Based on the current study, the mechanism of ATO-induced ceramide accumulation in ATL-derived cells was similar to that seen in APL-derived cells, and involved simultaneous activation of *de novo* ceramide synthesis and inhibition of ceramide metabolism through GCS. The combination of increased synthesis of ceramide and its decreased incorporation into more complex sphingolipids results in a more rapid and sustained accumulation of ceramide. In contrast, although various other chemotherapeutic agents have been shown to induce ceramide accumulation, most do so by activating a single pathway. This finding might help to explain the wide-ranging growth suppressive effects of ATO.

Remarkably, ATO induced significant *de novo* ceramide synthesis in ATL-derived HTLV-I-positive cells, known to be defective in this pathway due to the expression of the viral oncoprotein Tax, as reported previously.[37] Indeed, Tax expression was sufficient to partially inhibit the generation of ceramide through the *de novo* pathway in response to HPR, and to suppress ceramide synthase activity. This defect may explain, at least in part, the chemo-resistance of ATL cells and the demonstrated response to ATO. The mechanism of suppression of ceramide synthesis by Tax is unknown. *De novo* synthesis of ceramide is dependent on the activity of several enzymes including several ceramide synthases.[50] A major biological function of Tax protein is its ability to induce a constitutive high level of activity of the transcription factor NF-κB.[51] The possibility that NF-κB activation suppresses one or more of the enzymes involved in ceramide synthesis is currently being evaluated in our laboratory. Tax also represses the transcriptional activity of the tumor suppressor protein p53, which has been shown to be upstream of ceramide accumulation.[52] Interestingly, ATO can also act on p53 paralog proteins such as p73.[53,54] Of note, there was no statistical difference between ATO- and ATO/interferon-induced increases in sphingomyelin

mass, although both increases were statistically greater than that of the control (Figure 4B). Similarly, there was no statistical difference between ATO- and ATO/interferon-induced increases in ^{3}H-ceramide, although, again, both increases were statistically greater than that of the control (Figure 4B). We previously identified two ATO targets in HTLV-I-transformed cells: (i) an ATO-induced, interferon-independent shut-off of the NF-κB pathway and (ii) an ATO-triggered, interferon-enhanced, proteasomal degradation of the viral oncoprotein Tax.[23-25] It is likely that these two effects of ATO remove the impairment of *de novo* ceramide synthesis, resulting in ceramide accumulation and cell death, but their relative contribution remains to be determined. Indeed, HTLV-I-positive cells are sensitive to ceramide-induced cell killing once sufficient levels have been generated.

In conclusion, deregulation of ceramide metabolism by oncoproteins may act as an indicator of tumor cells and could be a target in cancer therapy. Understanding the nature of deregulation of these pathways in specific tumor types may help in identifying effective chemotherapeutic agents with known specific modulating effects on ceramide pathways. Arsenic treatment of APL and ATL-derived cells target similar metabolic pathways resulting in oncoprotein degradation and accumulation of cytotoxic levels of ceramide. This suggests that ATO-induced ceramide accumulation may represent a general intermediate mediator of the effects of ATO and paves the way for new therapeutic interventions that target the metabolic pathway of this important sphingolipid secondary messenger.

Authors' Contributions

All authors contributed to this study and to the writing of the final version of the manuscript.

Conflict of Interest

The authors reported no potential conflicts of interest.

References

1. Sanz MA, Fenaux P, Lo Coco F; European APL Group of Experts. Arsenic trioxide in the treatment of acute promyelocytic leukemia. A review of current evidence. Haematologica 2005;90:1231-5.
2. De The H, Chomienne C, Lanotte M, Degos L, Dejean A. The t(15;17) translocation of acute promyelocytic leukaemia fuses the retinoic acid receptor alpha gene to a novel transcribed locus. Nature 1990;347: 558–61.
3. Warrell RP Jr, de The H, Wang ZY, Degos L. Acute promyelocytic leukemia. N Engl J Med 1993;329: 177-89.
4. Fenaux P, Chastang C, Chevret S, Sanz M, Dombret H, Archimbaud E, et al. A randomized comparison of all transretinoic acid (ATRA) followed by chemotherapy and ATRA plus chemotherapy and the role of maintenance therapy in newly diagnosed acute promyelocytic leukemia. The European APL Group. Blood 1999;

94:1192-200.
5. Fenaux P, Le Deley MC, Castaigne S, Archimbaud E, Chomienne C, Link H, et al. Effect of all transretinoic acid in newly diagnosed acute promyelocytic leukemia. Results of a multicenter randomized trial. European APL 91 Group. Blood 1993;82:3241-9.
6. Tallman MS, Andersen JW, Schiffer CA, Appelbaum FR, Feusner JH, Woods WG, et al. All-trans retinoic acid in acute promyelocytic leukemia: long-term outcome and prognostic factor analysis from the North American Intergroup protocol. Blood 2002;100: 4298-302.
7. Shen ZX, Chen GQ, Ni JH, Li XS, Xiong SM, Qiu QY, et al. Use of arsenic trioxide (As₂O₃) in the treatment of acute promyelocytic leukemia (APL): II. Clinical efficacy and pharmacokinetics in relapsed patients. Blood 1997;89: 3354–60.
8. Soignet SL, Maslak P, Wang ZG, Jhanwar S, Calleja E, Dardashti LJ, et al. Complete remission after treatment of acute promyelocytic leukemia with

arsenic trioxide. N Engl J Med 1998; 339:1341-8.
9. Raffoux E, Rousselot P, Poupon J, Daniel MT, Cassinat B, Delarue R, et al. Combined treatment with arsenic trioxide and all-trans-retinoic acid in patients with relapsed acute promyelocytic leukemia. J Clin Oncol 2003;21: 2326-34.
10. Lallemand-Breitenbach V, Guillemin MC, Janin A, Daniel MT, Degos L, Kogan SC, et al. Retinoic acid and arsenic synergize to eradicate leukemic cells in a mouse model of acute promyelocytic leukemia. J Exp Med 1999;189:1043–52.
11. Estey E, Garcia-Manero G, Ferrajoli A, Faderl S, Verstovsek S, Jones D, et al. Use of all-trans retinoic acid plus arsenic trioxide as an alternative to chemotherapy in untreated acute promyelocytic leukemia. Blood 2006; 107:3469-73.
12. Mathews V, George B, Lakshmi KM, Viswabandya A, Bajel A, Balasubramanian P, et al. Single-agent arsenic trioxide in the treatment of newly diag-

nosed acute promyelocytic leukemia: durable remissions with minimal toxicity. Blood 2006;107:2627-32.

13. Ghavamzadeh A, Alimoghaddam K, Ghaffari SH, Rostami S, Jahani M, Hosseini R, et al. Treatment of acute promyelocytic leukemia with arsenic trioxide with ATRA and/or chemotherapy. Ann Oncol 2006;17: 131-4.

14. Zhu J, Chen Z, Lallemand-Breitenbach V, de The H. How acute promyelocytic leukaemia revived arsenic. Nat Rev Cancer 2002;2:705–13.

15. Zhu J, Koken M, Guignon F, Chelbi-Alix MK, Degos L, Yi Wang Z, et al. Arsenic-induced PML targeting onto nuclear bodies implications for the treatment of acute promyelocytic leukemia. Proc Natl Acad Sci USA 1997;94:3978-83.

16. Hinuma Y, Komoda H, Chosa T, Kondo T, Kohakura M, Takenaka T, et al. Antibodies to adult T-cell leukemia-virus-associated antigen (ATLA) in sera from patients with ATL and controls in Japan: a nation-wide sero-epidemiologic study. Int J Cancer 1982;29:631-5.

17. Shimoyama M. Treatment of patients with adult T-cell leukemia-lymphoma: an overview. In Takatsuki K, Hinuma Y, Yoshida M, editors. Advances in adult T-cell leukemia and HTLV-I research: Japan scientific societies press. In Takatsuki K 1992; p. 43-56.

18. Bazarbachi A, Ghez D, Lepelletier Y, Nasr R, de The H, El-Sabban ME, et al. New therapeutic approaches for adult T-cell leukaemia. Lancet Oncol 2004; 5:664-72.

19. Gill PS, Harrington W Jr, Kaplan MH, Ribeiro RC, Bennett JM, Liebman HA, et al. Treatment of adult T-cell leukemia-lymphoma with a combination of interferon α and zidovudine. N Engl J Med 1995;332:1744-8.

20. Hermine O, Bouscary D, Gessain A, Turlure P, LeBlond V, Franck N, et al. Brief report: treatment of adult T-cell leukemia-lymphoma with zidovudine and interferon α. N Engl J Med 1995; 332:1749-51.

21. Bazarbachi A, Hermine O. Treatment with a combination of zidovudine and α-interferon in naive and pretreated adult T-cell leukemia/lymphoma patients. J Acquir Immune Defic Syndr Hum Retrovirol 1996; 13 Suppl 1: S186-90.

22. Hermine O, Allard I, Levy V, Arnulf B, Gessain A, Bazarbachi A. French ATL therapy group. A prospective phase II clinical trial with the use of zidovudine and interferon-α in the acute and lymphoma forms of adult T-cell leukemia/lymphoma. Hematol J 2002;3: 276-82.

23. Bazarbachi A, El-Sabban ME, Nasr R, Quignon F, Awaraji C, Kersual J, et al. Arsenic trioxide and interferon-alpha synergize to induce cell cycle arrest and apoptosis in human T-cell lymphotropic virus type I-transformed cells. Blood 1999;93: 278-83.

24. El-Sabban ME, Nasr R, Dbaibo G, Hermine O, Abboushi N, Quiqnon F, et al. Arsenic-interferon-alpha-triggered apoptosis in HTLV-I transformed cells is associated with tax down-regulation and reversal of NF-kappa B activation. Blood 2000;96: 2849-55.

25. Nasr R, Rosenwald A, El-Sabban ME, Arnulf B, Zalloua P, Lepelletier Y, et al. Arsenic/interferon specifically reverses two distinct gene networks critical for the survival of HTLV-I infected leukemic cells. Blood 2003;101:4576-82.

26. Hermine O, Dombret H, Poupon J, Arnulf B, Lefrere F, Rousselot P, et al. Phase II trial of arsenic trioxide and α interferon in patients with relapsed/refractory adult T-cell leukemia/lymphoma. Hematol J 2004;5:130-4.

27. Hannun YA. The sphingomyelin cycle and the second messenger function of ceramide. J Biol Chem 1994;269: 3125-8.

28. Hannun YA. Functions of ceramide in coordinating cellular responses to stress. Science 1996;274:1855-9.

29. Cai Z, Bettaieb A, Mahdani NE, Legres LG, Stancou R, Masliah J, et al. Alteration of the sphingomyelin/ceramide pathway is associated with resistance of human breast carcinoma MCF7 cells to tumor necrosis factor-α-mediated cytotoxicity. J Biol Chem 1997;272:6918-26.

30. Michael JM, Lavin MF, Watters DJ. Resistance to radiation-induced apoptosis in Burkitt's lymphoma cells is associated with defective ceramide signaling. Cancer Res 1997;57:3600-5.

31. Chmura SJ, Mauceri HJ, Advani S, Heimann R, Beckett MA, Nodzenski E, et al. Decreasing the apoptotic threshold of tumor cells through protein kinase C inhibition and sphingomyelinase activation increases tumor killing by ionizing radiation. Cancer Res 1997;57:4340-7.

32. Lavie Y, Cao H, Volner A, Lucci A, Han TY, Geffen V, et al. Agents that reverse multidrug resistance, tamoxifen, verapamil, and cyclosporine A, block glycosphingolipid metabolism by inhibiting ceramide glycosylation in human cancer cells. J Biol Chem 1997;272: 1682-7.

33. Bielawska A, Crane HM, Liotta D, Obeid LM, Hannun YA. Selectivity of ceramide-mediated biology. Lack of activity of erythro-dihydroceramide. J Biol Chem 1993;268: 26226-32.

34. Andrieu-Abadie N, Gouaze V, Salvayre R, Levade T. Ceramide in apoptosis signaling: relationship with oxidative stress. Free Radic Biol Med 2001;31:717-28.

35. Perry DK, Bielawska A, Hannun YA. Quantitative determination of ceramide using diglyceride kinase. Methods Enzymol 2000;312:22-31.

36. Murate T, Suzuki M, Hattori M, Takagi A, Kojima T, Tanizawa T, et al. Up-regulation of acid sphingomyelinase during retinoic acid-induced myeloid differentiation of NB4, a human acute promyelocytic leukemia cell line. J Biol Chem 2002; 277:9936-43.

37. Darwiche N, Abou-Lteif G, Najdi T, Kozhaya L, Abou Tayyoun A, Bazarbachi A, et al. Human T-cell lymphotropic virus type I-transformed T cells have a partial defect in ceramide synthesis in response to N-(4-hydroxyphenyl) retinamide. Biochem J 2005; 392:231-9.

38. Lanotte M, Martin-Thouvenin V, Najman S, Balerini P, Valensi F, Berger R. NB4, a maturation inducible cell line with t(15;17) marker isolated from a human acute promyelocytic leukemia (M3). Blood 1991;77:1080-6.

39. Bligh EG, Dyer WJ. A rapid method of total lipid extraction and purification. Can J Bioch Phys 1959; 37:911-7.

40. Bielawska A, Perry DK, Hannun YA. Determination of ceramides and diglycerides by the diglyceride kinase assay. Anal Biochem 2001; 298:141-50.

41. Perry DK. The role of de novo ceramide synthesis in chemotherapy-induced apoptosis. Ann NY Acad Sci 2000;905:91-6.

42. Liu YY, Han TY, Giuliano AE, Cabot MC. Expression of glucosylceramide synthase, converting ceramide to glucosylceramide, confers adriamycin resistance in human breast cancer cells. J Biol Chem 1999;274:1140-6.

43. Ogretmen B, Pettus BJ, Rossi MJ, Wood R, Usta J, Szulc Z, et al. Biochemical mechanisms of the generation of endogenous long chain ceramide in response to exogenous short chain ceramide in the A549 human lung adenocarcinoma cell line. Role for endogenous ceramide in mediating the action of exogenous ceramide. J Biol Chem 2002; 277: 12960-9.

44. Okazaki T, Bielawska A, Bell RM, Hannun YA. Role of ceramide as a lipid mediator of 1α,25-dihydroxyvitamin D3-induced HL-60 cell differentiation. J Biol Chem 1990;265: 15823-31.

45. Jayadev S, Liu B, Bielawska AE, Lee JY, Nazaire F, Pushkareva M, et al. Role for ceramide in cell cycle arrest. J Biol Chem 1995;270:2047-52.

46. Dbaibo GS, Pushkareva MY, Jayadev S, Schwarz JK, Horowitz JM, Obeid LM, et al. Retinoblastoma gene product as a downstream target for a ceramide-dependent pathway of growth arrest. Proc Natl Acad Sci USA 1995;92:1347-51.

47. Obeid LM, Linardic CM, Karolak LA, Hannun YA. Programmed cell death induced by ceramide. Science 1993; 259:1769-71.

48 Venable ME, Lee JY, Smyth MJ, Bielawska A, Obeid LM. Role of ceramide in cellular senescence. J Biol Chem 1995;270:30701-8.

49. Hannun YA, Luberto C. Ceramide in the eukaryotic stress response. Trends Cell Biol 2000;10:73-80.

50. Futerman AH, Riezman H. The ins and outs of sphingolipid synthesis. Trends Cell Biol 2005;15:312-8.

51. Kfoury Y, Nasr R, Hermine O, de The H, Bazarbachi A. Proapoptotic regimes for HTLV-I-transformed cells: targeting Tax and the NF-kappaB pathway. Cell Death Differ 2005; 12 Suppl 1:871-7.

52. Dbaibo GS, Pushkareva MY, Rachid RA, Alter N, Smyth MJ, Obeid LM, et al. p53-dependent ceramide response to genotoxic stress. J Clin Invest 1998; 102:329-39.

53. Lunghi P, Costanzo A, Levrero M, Bonati A. Treatment with arsenic trioxide (ATO) and MEK1 inhibitor activates the p73-p53AIP1 apoptotic pathway in leukemia cells. Blood 2004; 104:519-25.

54. Lunghi P, Costanzo A, Salvatore L, Noguera N, Mazzera L, Tabilio A, et al. MEK1 inhibition sensitizes primary acute myelogenous leukemia to arsenic trioxide–induced apoptosis. Blood 2006;107:4549-53.